Osthole inhibits the tumorigenesis of hepatocellular carcinoma cells

ZHI-KUN LIN[1*], JIA LIU[2*], GUO-QIANG JIANG[2*], GUANG TAN[1], PENG GONG[1], HAI-FENG LUO[1],
HUI-MIN LI[3], JIAN DU[1], ZHEN NING[1], YI XIN[2] and ZHONG-YU WANG[1]

[1]Department of Hepatobiliary Surgery, The First Affiliated Hospital of Dalian Medical University;
Departments of [2]Biotechnology and [3]Histology and Embryology, Dalian Medical University,
Dalian, Liaoning 116011, P.R. China

Abstract. Hepatocellular carcinoma (HCC) accounts for approximately 90% of all cases of primary liver cancer, and the majority of patients with HCC are deprived of effective curative methods. Osthole is a Chinese herbal medicine which has been reported to possess various pharmacological functions, including hepatocellular protection. In the present study, we investigated the anticancer activity of osthole using HCC cell lines. We found that osthole inhibited HCC cell proliferation, induced cell cycle arrest, triggered DNA damage and suppressed migration in HCC cell lines. Furthermore, we demonstrated that osthole not only contributed to cell cycle G2/M phase arrest via downregulation of Cdc2 and cyclin B1 levels, but also induced DNA damage via an increase in ERCC1 expression. In addition, osthole inhibited the migration of HCC cell lines by significantly downregulating MMP-2 and MMP-9 levels. Finally, we demonstrated that osthole inhibited epithelial-mesenchymal transition (EMT) via increasing the expression of epithelial biomarkers E-cadherin and β-catenin, and significantly decreasing mesenchymal N-cadherin and vimentin protein expression. These results suggest that osthole may have potential chemotherapeutic activity against HCC.

Introduction

Hepatocellular carcinoma (HCC) is a common tumor type with high metastatic ability and recurrence rate (1,2). HCC has a higher incidence in developing countries compared with that in developed countries and the highest incidence rates are found in China (3). Worlwide, HCC is the fifth most commonly diagnosed cancer, but the second most leading cause of cancer-related death (3). Some patients are deprived of the opportunity of curative therapy due to advanced stage disease, and systemic chemotherapy has shown little benefit on the survival rate of patients (4,5). Therefore, the underlying mechanisms of cancer cell migration, invasion and proliferation must be thoroughly elucidated to provide critical signaling effectors for effective molecularly targeted therapy.

Osthole (Fig. 1A), a herbal medicine, is a simple bioactive [7-methoxy-8-(3methy-2-butenyl)] coumarin derivative. It has been proven to exhibit various pharmacological functions. It is an anticonvulsant (6), prevents ischemia-reperfusion injury (7), has hepatocellular protective properties (8) and has anti-allergic function (9). Research on the effect of osthole on HCC is lacking, yet a few studies have reported that osthole possesses anticancer potential, and was found to inhibit the growth of human glioma (10), induce apoptosis in human lung cancer and human osteosarcoma (11,12), and inhibit metastasis in human glioblastoma and human lung cancer (13,14). In HCC, osthole was reported to play a crucial role in growth inhibition and induction of apoptosis (15), but it is unclear whether osthole has influence on HCC migration and invasion as well as critical signaling pathways.

In the present study, we demonstrated for the first time the pharmacological function of osthole in inducing cell cycle arrest through downregulation of cycle B1 and Cdc2 levels and in triggering DNA damage through upregulation of ERCC1 and we further elucidated its effects on HCC cell migration associated with a decrease in MMP-9 and MMP-2 expression and modulating the epithelial-mesencheymal transition (EMT) signaling pathway.

Materials and methods

Materials, reagents and chemicals. Antibodies against MMP-2, MMP-9, Cdc2, cyclin B1, β-catenin, E-cadherin, vimentin and β-actin were obtained from ProteinTech Group, Inc. (Chicago, IL, USA), and the antibody for N-cadherin was obtained Cell Signaling Technology, Boston, MA, USA). An enhanced chemiluminescence (ECL) kit was purchased from Amersham Life Sciences, Inc. (Piscataway, NJ, USA).

Correspondence to: Dr Zhong-Yu Wang, Department of Hepatobiliary Surgery, The First Affiliated Hospital of Dalian Medical University, 222 Zhongshan Road, Dalian, Liaoning 116011, P.R. China
E-mail: fishflowers@hotmail.com

Dr Yi Xin, Department of Biotechnology, Dalian Medical University, 9 West Lushun South Road, Dalian, Liaoning 116011, P.R. China
E-mail: jimxin@hotmail.com

*Contributed equally

Cell cycle detection and comet assay kits were purchased from Nanjing KeyGen Biotech Co., Ltd. (Nanjing, China). Transwells were obtained from BD Biosciences (San Jose, CA, USA). 3-(4,5-Dimethylthiazole-2-yl)-2,5-diphenyltetrazolium bromide (MTT) and dimethyl sulfoxide (DMSO) were obtained from Sigma Chemical Co. (St. Louis, MO, USA). Osthole powder was purchased from Chengdu Must Bio-Technology Co., Ltd. (Chengdu, China). It contained ~98% proanthocyanidins and is stable for at least two years at 4°C.

Cell lines and cell culture. The HCC, SMCC-7721, MHCC-97H, HCC-LM3 and BEL-7402 cell lines were obtained from the Cell Bank of the Chinese Academy of Sciences (Shanghai, China), and were cultured in Dulbecco's modified Eagle's medium (DMEM) supplemented with 10% fetal bovine serum (FBS) and 100 U/ml penicillin (all from Gibco-BRL, Grand Island, NY, USA) at 37°C with 5% CO_2 in a humidified incubator.

Drug preparation. Osthole was dissolved in 100% DMSO at a concentration of 1 M as a stock solution and stored at 4°C. It was diluted with DMEM before each experiment. The final concentrations of DMSO were <0.1% in all osthole treatment groups.

Cell viability assay. The effect of osthole on cell viability was detected using the MTT assay. The cells ($1x10^4$/well) were seeded into a 96-well plate and incubated for 24 h. After treatment with osthole (20, 40, 80, 120, 160 or 200 μM) and the negative control for 24 and 48 h, the viability of the cancer cells was detected with MTT. Twenty microliters of MTT solution [5 mg/ml in phosphate-buffered saline (PBS)] was added to each well, and the mixtures were incubated for 4 h at 37°C. Then, the MTT solution was removed and 150 μl of DMSO was added to the wells. The absorbance was measured using a Multiskan Ascent plate reader at a 540 nm wavelength.

Cell cycle analysis by flow cytometry. Cell cycle progression was assayed by measuring DNA content with propidium iodide (PI) staining. The cells were treated with osthole (0, 80, 120 or 160 μM) for 24 h, washed twice with PBS and fixed with 70% ethanol overnight at 4°C. Following fixation, the DNA fragments were stained in PBS containing PI and RNase for 1 h at 37°C. The DNA content was evaluated using an Accuri C6 flow cytometer (BD Biosciences). The data were analyzed using ModFit LT V4.1.

Wound healing assay. SMCC-7721 and MHCC-97H cells were seeded into 24-well plates and scraped with the end of a 200-μl pipette tip. The plates were washed with PBS to remove detached cells, and then the cells were incubated with complete growth medium containing 0, 20 and 40 μM osthole solution for 24 h. Cell migration was observed under a phase-contrast microscope at a magnification of x100 field at 0 and 24 h post-induction of injury. Migrated cells into the denuded area in each of six random fields were measured and quantified with computer-assisted microscope.

Transwell migration assay. Cell migration and invasion were quantified by the Transwell assay. HCC cells were treated with 0, 20 and 40 μM osthole for 24 h and harvested. Cells ($2x10^4$) in serum-free DMEM were added to each upper chamber and DMEM with 10% FBS was added to the lower chamber as a chemoattractant. After a 24-h incubation at 37°C, the cells remaining on the upper surface of the membrane were removed, and the cells that had migrated through the membrane were stained with 0.1% crystal violet for 10 min. Six random fields of each Transwell membrane were assessed under a light microscope at a magnification of x200.

Comet assay for the analysis of DNA damage. DNA damage induced by osthole in the HCC cells was determined using a comet assay according to the manufacturer's protocol. Briefly, cells were treated with osthole (80 and 120 μM) for 48 h in complete medium, and then the cells were harvested and re-suspended in ice-cold PBS buffer. Approximately $1x10^4$ cells in a volume of 75 μl of 0.5% (w/v) low-melting-point agarose were pipetted into a frosted glass slide coated with a thin layer of 1.0% (w/v) agarose, covered with a coverslip, and allowed to set on ice for 10 min. Coverslips were removed, and the slides were immersed in ice-cold lysis buffer. After 2 h at 4°C, the slides were placed into a horizontal electrophoresis tank filled with electrophoresis buffer and subjected to electrophoresis for 30 min at 30 V at 4°C. Cells were stained with 2.5 μg/ml PI for 5 min and visualized under a microscope at a magnification of x200 field. Tail lengths of a minimum of 10 cells were quantified as the distance from the center of the cell nucleus to the tip of the tail.

Western blot analysis. Protein was extracted using RIPA lysis buffer (Beyotime, Shanghai, China) and protease inhibitor (Biocolors, Shanghai, China) was added in a proportion of 1:100. Equal amount of protein was loaded on a 10% SDS-PAGE gel. The lysates were resolved by electrophoresis (80 V for 30 min and 120 V for 1.5 h) and transferred onto polyvinylidene difluoride (PVDF) membranes. The membranes were blocked in 5% non-fat milk for 1 h at room temperature and incubated with the primary antibody overnight at 4°C, followed by incubation with relevant secondary antibodies for 1 h at room temperature. The protein bands were visualized using the chemiluminescent ECL assay kit (Amersham Life Sciences, Inc.) and images were captured using Bio-Rad ChemiDoc XRS. Protein expression was quantitatively determined using ImageJ software (National Institutes of Health, Bethesda, MD, USA). β-actin was used as an internal reference for protein expression in all cells.

Statistical analysis. Data were analyzed using SPSS 15.0 software and are presented as means ± SD of three independent experiments. Statistical differences between two groups were analyzed using a Student's t-test. A difference was considered to be statistically significant at P<0.05.

Results

Effect of osthole on the proliferation of HCC cells. Human HCC cell lines SMCC-7721, BEL-7402, MHCC-97H and HCC-LM3, and a normal cell line LO2 were incubated with different concentrations (0, 20, 40, 80, 120, 160 and 200 μM) of osthole for 24 and 48 h (Fig. 1B), and then the cell viability
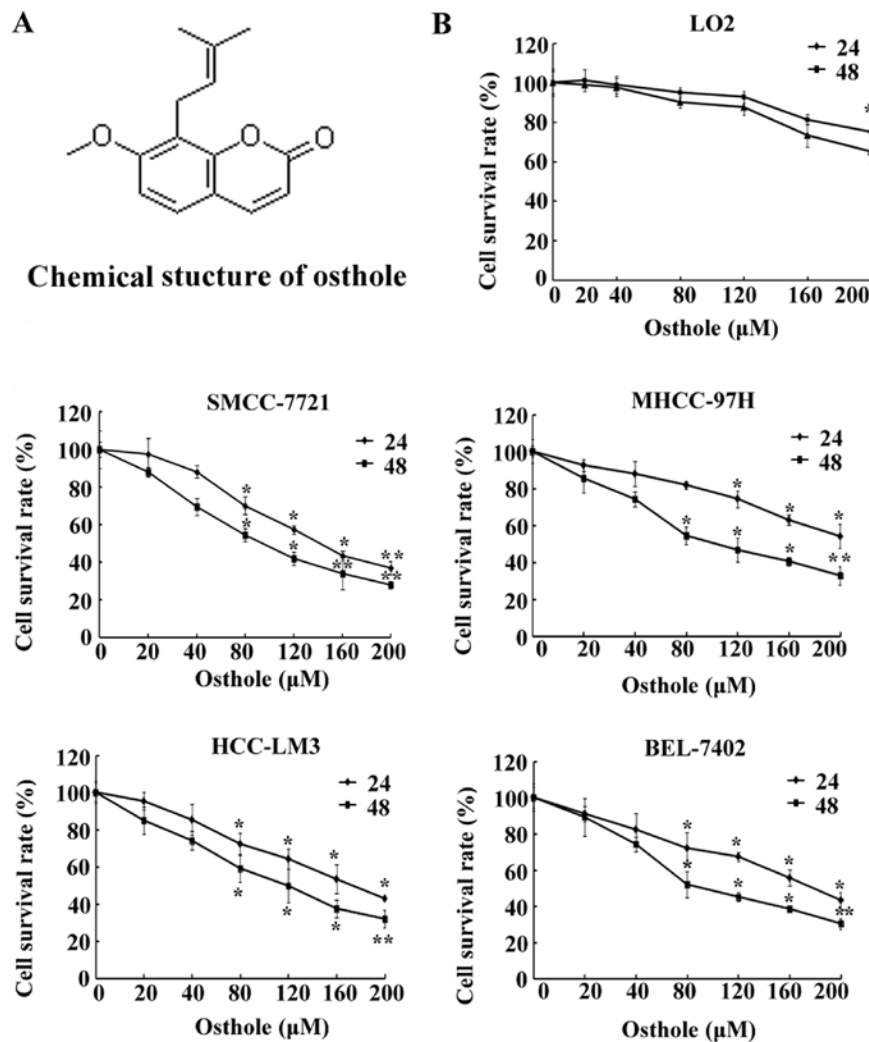
Figure 1. Effect of osthole on the proliferation of hepatocellular carcinoma cells. (A) Chemical structure of osthole. (B) Cell viability was measured by MTT assay in hepatocellular carcinoma cell lines SMCC-7721, MHCC-97H, HCC-LM3 and BEL-7402 and normal cell line LO2 following treatment with osthole (0, 20, 40, 80, 120, 160 and 200 µM) for 24 and 48 h. *P<0.01 and **P<0.001, significant differences compared to the control group.

was determined by MTT assay. As shown in Fig. 1B, except for the MHCC-97H cell line, incubation with osthole at 80 µM for 24 h significantly inhibited HCC cell proliferation, and following 48 h of treatment with osthole at 80 µM marked effects were noted on the inhibiton of cell growth. However, a concentration of 120 µM oshole had a marked significant effect on the inhibition of cell growth. Additionally, HCC cell lines following osthole treatment demonstrated a significant decrease in cell viability in a dose- and time-dependent manner (P<0.05), while the same concentrations did not significantly affect the viability of the normal LO2 cells.

Osthole induces cell G2/M phase arrest in HCC cell lines. To examine whether osthole contributes to the induction of cell cycle arrest, the effect on the cell cycle was measured by flow cytometry. HCC cell lines were treated with osthole at different concentrations (0, 80, 120 and 160 µM) for 24 h and the SMCC-7721 and MHCC-97H cell lines exhibited significantly increased accumulation of cells in the G2/M phase after osthole incubation for 24 h, whereas osthole did not significantly affect the S phase (Fig. 2A). Along with increasing

concentrations, the percentages of cells in the G2/M phase were markedly increased from 16.8% (control group) to 64.32% in the SMCC-7721 cells, and from 4.52% (control group) to 41.48% in the MHCC-97H cells (Fig. 2B), indicating that osthole was able to induce cell cycle arrest in the G2/M phase in a dose-dependent manner. The proportion of apoptotic cells increased with increasing concentrations of osthole (Fig. 2B).

DNA damage by osthole in HCC cell lines. The degree of DNA damage was evaluated by the comet assay after the HCC SMCC-7721 and MHCC-97H cell lines were exposed to osthole at various concentrations (0, 80 and 120 µM) for 24 h, respectively. The representative images of DNA damage acquired from the comet assay are presented in Fig. 3, which shows that the comet tail was significantly extended compared to the control group and DNA damage was increased with the increasing concentration of osthole, suggesting that osthole triggered DNA damage in a dose-dependent manner.

Osthole inhibits the migration of HCC cells. The effect of osthole on HCC cell migration was evaluated by Transwell
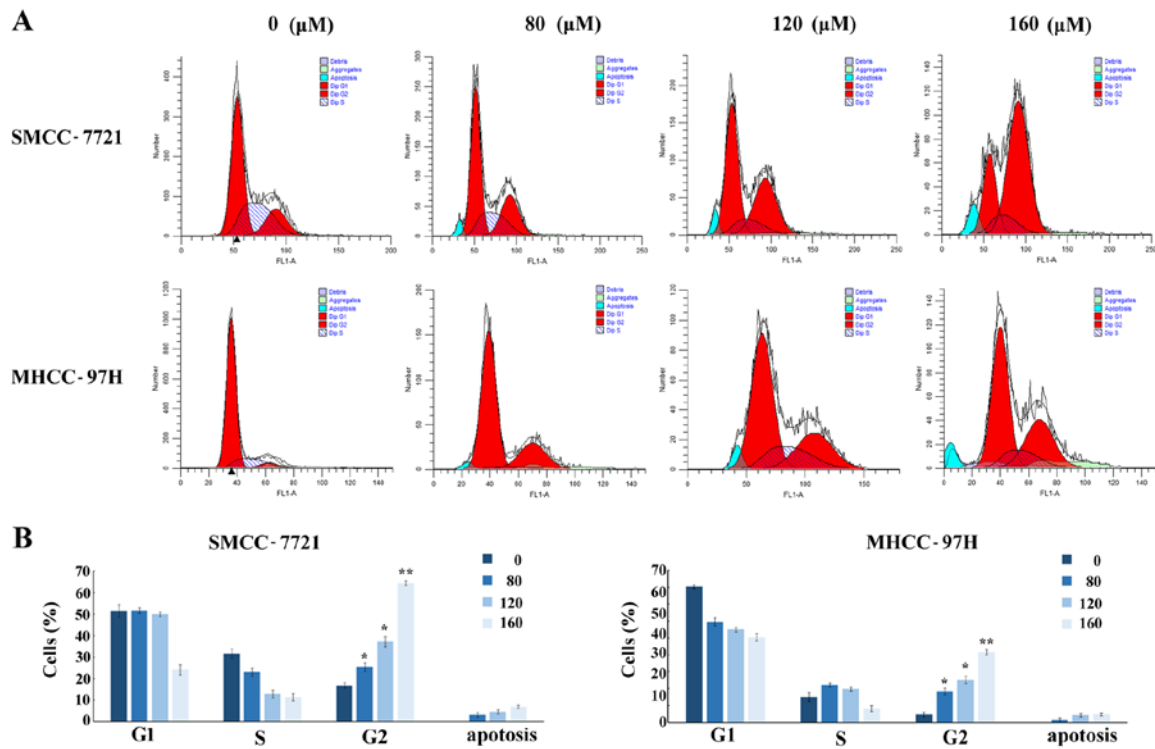
Figure 2. Analysis of cell cycle distribution by flow cytometry. (A) Cell cycle analysis of SMCC-7721 and MHCC-97H cells following treatment with 0, 80, 120 and 160 μM osthole for 24 h by flow cytometry. (B) The percentages of cells in the G1/G0, S, G2/M phases and apoptotic phase are shown in the histograms; *P<0.01 and **P<0.001 compared to the control group. Data are presented as means ± SD of three independent experiments. For each independent experiment, the assays were performed in duplicate.
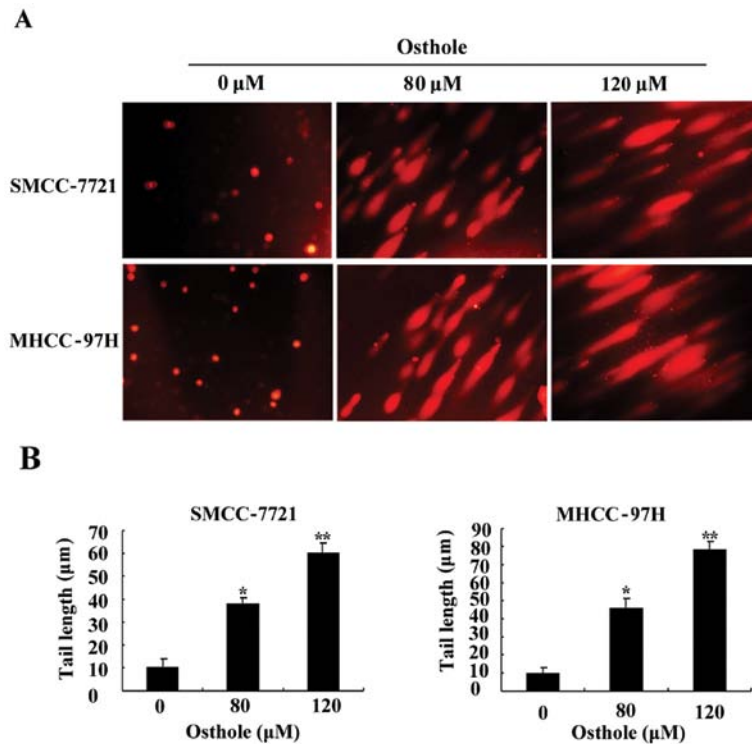

Figure 3. Osthole induces strand breaks in cellular DNA of hepatocellular carcinoma cells. (A) DNA damage was measured using comet assay in the SMCC-7721 and MHCC-97H cells following treatment with different concentrations of osthole (0, 80 and 120 μM). (B) The tail length of each comet was measured in each cell and tail length is expressed in μm as mean ± SD from at least 10 cells in each treatment group; *P<0.01 and **P<0.001 compared to the control group.

and wound healing assays in the SMCC-7721 and MHCC-97H cell lines following treatment with different concentrations (0, 20 and 40 μM) of osthole for 24 h, which were not apoptotic. As shown in Fig. 4A and B, the mobility ratio of HCC cells
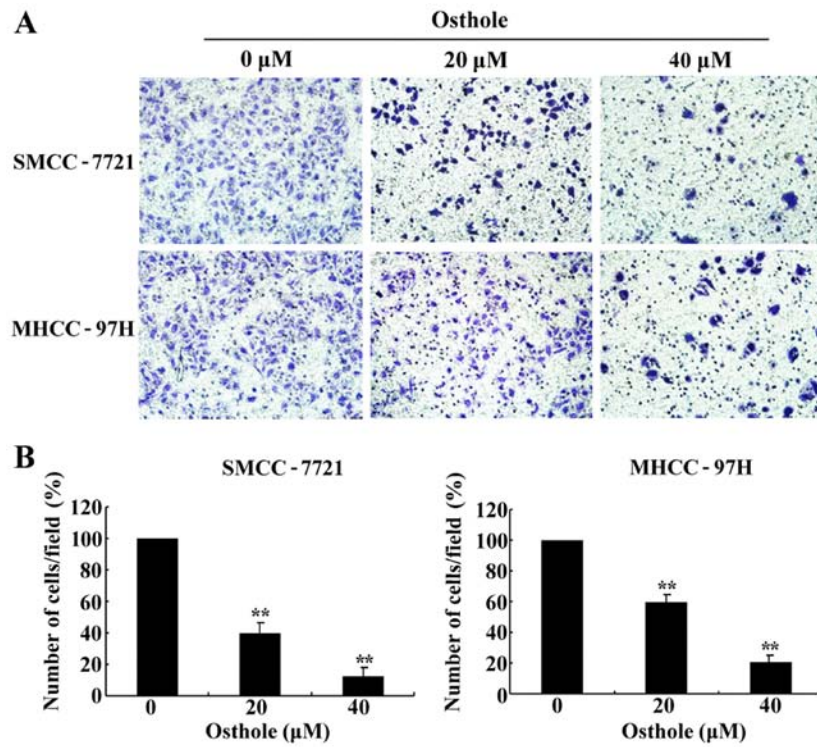
Figure 4. Effect of osthole on the migration of hepatocellular carcinoma cells by Transwell assay. (A) Representative images of cell migration onto the underside of the Transwell membrane under a microscope at a magnification of x200 field after cells were treated with osthole (0, 20 and 40 μM) for 24 h. (B) Average cell number of each field was counted. Migrated cells are expressed relative to that of the control group. The experiments were repeated three times; [**]P<0.001 compared to the control group.
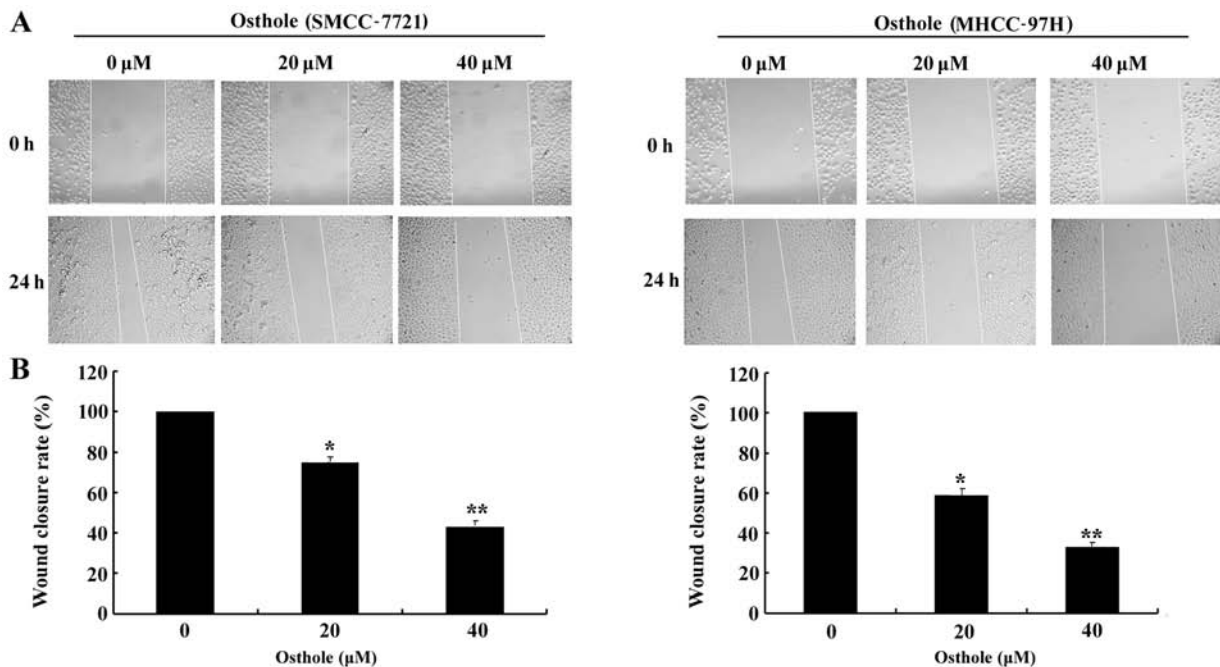

Figure 5. Effects of osthole on the migration of hepatocellular carcinoma cells by wound healing assay. Cells were treated with osthole (0, 20 and 40 μM) for 24 h. (A) Representative images of cell migration in the wound healing assay under a microscope at a magnification of x100 field before and after injury. (B) The migration of SMCC-7721 and MHCC-97H cells was quantified by measuring wound closure areas before and after injury. The experiments were repeated three times; [*]P<0.01 and [**]P<0.001 compared to the control group.

from the upper to the lower chamber gradually declined along with increased concentrations of osthole. Then, we performed a wound healing assay (Fig. 5). The wound closure rate of

the osthole-incubated cells was lower than that of the control group (Fig. 5B). The results revealed that osthole significantly inhibited HCC cell migration in a dose-dependent manner,
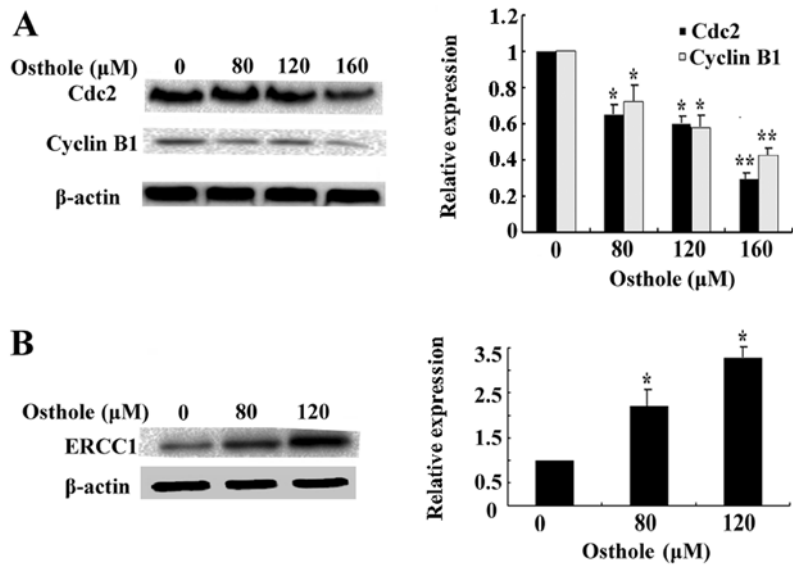
Figure 6. Effects of osthole on cell cycle- and DNA damage-related protein expression. (A) Cdc2 and cyclin B1 protein expression was assessed using western blotting in SMCC-7721 cells following treatment with osthole (0, 80,120 and 160 μM) for 24 h. (B) ERCC1 protein expression was assessed using western blotting in SMCC-7721 cells following treatment with osthole (0, 80 and 120 μM) for 24 h; statistical analysis of quantification is shown; *P<0.01 and **P<0.001 compared to the control group.
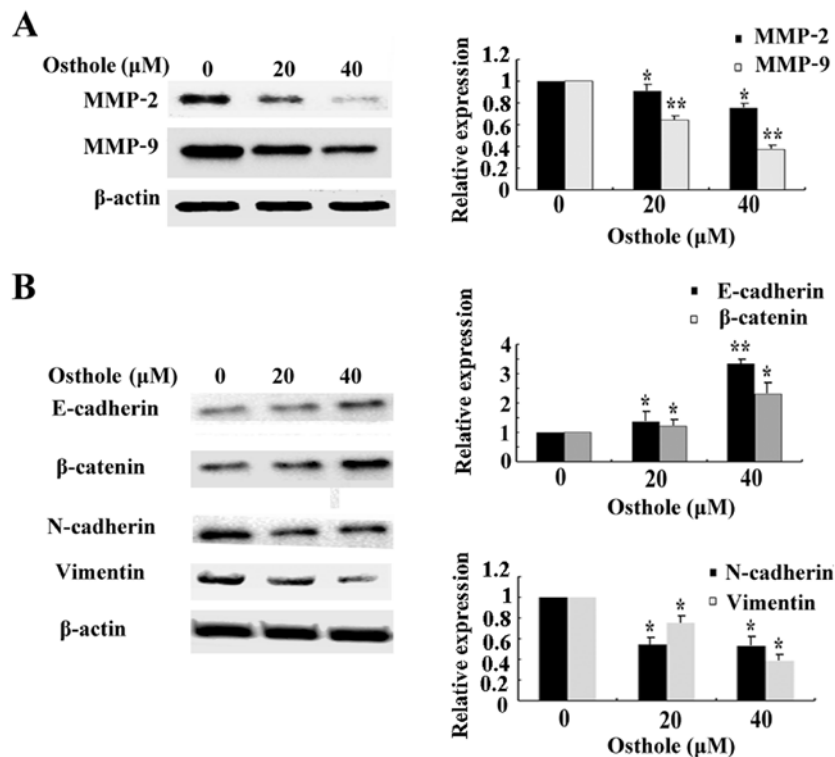

Figure 7. Effects of osthole on EMT- and migration-related protein expression. SMCC-7721 cells were treated with osthole (0, 20 and 40 μM) for 24 h. (A) The expression levels of migration-related proteins MMP-2 and MMP-9 were assessed by western blotting. (B) Protein expression was analyzed by western blotting for epithelial markers E-cadherin and β-catenin and mesenchymal proteins N-cadherin and vimentin; statistical analysis of quantification is shown; *P<0.01 and **P<0.001 compared to the control group.

suggesting a critical role for osthole in the inhibition of HCC cell metastasis.

Effects of osthole on cell cycle-, DNA damage-, EMT- and migration-related protein expression. To further confirm the underlying molecular mechanisms of the induction of

G2/M phase arrest by osthole, we examined the expression of cell cycle marker proteins Cdc2 and cyclin B1. As shown in Fig. 6A, the expression levels of Cdc2 and cyclin B1 were decreased following treatment with increasing concentrations of osthole. Then, we investigated the level of DNA damage marker protein ERCC1. As shown in Fig. 6B, the level of

ERCC1 was significantly upregulated after treatment with osthole in a dose-dependent manner. Finally, we assessed the expression of migration-related proteins MMP-2 and MMP-9 after cells were exposed to osthole. As shown in Fig. 7A, along with increasing concentrations of osthole, the expression of MMP-2 and MMP-9 was gradually decreased. Osthole also increased the expression of epithelial markers, E-cadherin and β-catenin, and significantly decreased expression of mesenchymal markers, N-cadherin and vimentin (Fig. 7B). These results indicate the potential link between osthole and HCC cell G2/M phase arrest, DNA damage, EMT and migration-related protein expression, and also confirmed our previous results on the pharmacological functions of osthole in HCC cells.

Discussion

Frequent patient diagnosis at advanced stage disease and limited effective treatment options contribute to the high mortality of HCC. In-depth knowledge of the multistep process leading to hepatocarcinogenesis, and development of novel chemotherapy targeting crucial signaling pathways may effectively improve the overall survival of patients with HCC across different stages (4). Osthole has been widely investigated due to its varied pharmacological functions (6,8,15-20). It has been reported that osthole inhibited ovarian cancer cells *in vitro* (19). We used concentrations from 0 to 200 μM to detect its effect on inhibition of cell proliferation. Our data confirmed that osthole induced cell cycle G2/M phase arrest and triggered DNA damage in HCC cell lines. Moreover, osthole significantly inhibited cell migration in HCC cells and we clarified the underlying mechanisms of these functions.

Dysregulated cell cycle and DNA damage response are currently two principal mechanisms of anticancer drugs (21,22). Cell cycle arrest as a critical target to inhibit cell proliferation has been widely investigated in recent years. Cdc2 and cyclin B1 are key regulators that modulate the G2/M checkpoint for cancer therapy (11,23-25). Furthermore, our results showed that osthole induced G2/M phase arrest in SMCC-7721 and MHCC-97H cells. Then, we demonstrated that treatment with osthole led to the downregulation of Cdc2 and cyclin B1 levels. Several studies have illustrated that osthole inhibited cancer cell proliferation and growth by cell cycle arrest (11,26). Suggesting that the underlying mechanism of osthole-induced HCC cell G2/M arrest may occur by attenuating the expression of Cdc2 and cyclin B1, this result is consistent with a previous study in lung cancer (11). In contrast, after incubation with osthole, DNA damage was significantly detected. Excision cross-complementation group 1 (ERCC1) has been found to be involved in DNA damage repair (27,28), and we found that ERCC1 was markedly upregulated in the experiment. Thus, we can conclude that osthole triggers DNA damage in HCC cell lines.

A great number of studies have focused on cancer cell metastasis due to its advanced threat to cancer patients. Increased expression of matrix metalloproteinases (MMPs) contributes to cancer cell migration, invasion and angiogenesis. MMP-2 and MMP-9 belong to the family of MMPs that have been widely studied (29-31). The EMT signaling pathway is also associated with cancer metastasis (32-34), and inhibition of EMT could be a potential therapeutic target to fight cancer metastasis. Previous research revealed that osthole inhibited cancer cell migration and invasion, in osteosarcoma, breast and lung cancer (26,35,36). In the present study, we demonstrated that osthole inhibited HCC cell migration in a dose-dependent manner, and we also further elucidated the underlying mechanisms by which osthole inhibits HCC cell migration by downregulating MMP-2 and MMP-9 expression and suppressing EMT by increasing the expression of epithelial markers, E-cadherin and β-catenin while decreasing mesenchymal markers, N-cadherin and vimentin.

Taken together, osthole possessed potential anticancer effects on HCC cells by inhibiting cell growth, inducing cell G2/M phase arrest, triggering DNA damage and suppressing migration *in vitro*. The underlying mechanisms of these functions were associated with the dysregulated expression of multiple proteins including Cdc2, cyclin B1, ERCC1, MMP-2, MMP-9, E-cadherin, β-catenin, N-cadherin and vimentin. We confirmed the potential pharmacological functions of osthole against HCC and elucidated the various mechanisms underlying these effects, suggesting that osthole may have high application value in HCC therapy.

References

1. Li H, Ge C, Zhao F, Yan M, Hu C, Jia D, Tian H, Zhu M, Chen T, Jiang G, *et al*: Hypoxia-inducible factor 1 alpha-activated angiopoietin-like protein 4 contributes to tumor metastasis via vascular cell adhesion molecule-1/integrin β1 signaling in human hepatocellular carcinoma. Hepatology 54: 910-919, 2011.
2. Zhang S, Yue M, Shu R, Cheng H and Hu P: Recent advances in the management of hepatocellular carcinoma. J BUON 21: 307-311, 2016.
3. Torre LA, Bray F, Siegel RL, Ferlay J, Lortet-Tieulent J and Jemal A: Global cancer statistics, 2012. CA Cancer J Clin 65: 87-108, 2015.
4. Liu CY, Chen KF and Chen PJ: Treatment of Liver Cancer. Cold Spring Harb Perspect Med 5: a021535, 2015.
5. Verslype C, Van Cutsem E, Dicato M, Arber N, Berlin JD, Cunningham D, De Gramont A, Diaz-Rubio E, Ducreux M, Gruenberger T, *et al*: The management of hepatocellular carcinoma. Current expert opinion and recommendations derived from the 10th World Congress on Gastrointestinal Cancer, Barcelona, 2008. Ann Oncol 20 (Suppl 7): vii1-vii6, 2009.
6. Luszczki JJ, Andres-Mach M, Cisowski W, Mazol I, Glowniak K and Czuczwar SJ: Osthole suppresses seizures in the mouse maximal electroshock seizure model. Eur J Pharmacol 607: 107-109, 2009.
7. Xie DQ, Sun GY, Zhang XG and Gan H: Osthole preconditioning protects rats against renal ischemia-reperfusion injury. Transplant Proc 47: 1620-1626, 2015.
8. Yu HP, Liu FC, Tsai YF and Hwang TL: Osthole attenuates hepatic injury in a rodent model of trauma-hemorrhage. PLoS One 8: e65916, 2013.
9. Matsuda H, Tomohiro N, Ido Y and Kubo M: Anti-allergic effects of Cnidii monnieri fructus (dried fruits of *Cnidium monnieri*) and its major component, osthol. Biol Pharm Bull 25: 809-812, 2002.
10. Lin K, Gao Z, Shang B, Sui S and Fu Q: Osthole suppresses the proliferation and accelerates the apoptosis of human glioma cells via the upregulation of microRNA-16 and downregulation of MMP-9. Mol Med Rep 12: 4592-4597, 2015.
11. Xu X, Zhang Y, Qu D, Jiang T and Li S: Osthole induces G2/M arrest and apoptosis in lung cancer A549 cells by modulating PI3K/Akt pathway. J Exp Clin Cancer Res: 30: 33, 2011.

12. Ding Y, Lu X, Hu X, Ma J and Ding H: Osthole inhibits proliferation and induces apoptosis in human osteosarcoma cells. Int J Clin Pharmacol Ther 52: 112-117, 2014.
13. Tsai CF, Yeh WL, Chen JH, Lin C, Huang SS and Lu DY: Osthole suppresses the migratory ability of human glioblastoma multiforme cells via inhibition of focal adhesion kinase-mediated matrix metalloproteinase-13 expression. Int J Mol Sci 15: 3889-3903, 2014.
14. Xu XM, Zhang Y, Qu D, Feng XW, Chen Y and Zhao L: Osthole suppresses migration and invasion of A549 human lung cancer cells through inhibition of matrix metalloproteinase-2 and matrix metallopeptidase-9 *in vitro*. Mol Med Rep 6: 1018-1022, 2012.
15. Zhang L, Jiang G, Yao F, He Y, Liang G, Zhang Y, Hu B, Wu Y, Li Y and Liu H: Growth inhibition and apoptosis induced by osthole, a natural coumarin, in hepatocellular carcinoma. PLoS One 7: e37865, 2012.
16. Ko FN, Wu TS, Liou MJ, Huang TF and Teng CM: Vasorelaxation of rat thoracic aorta caused by osthole isolated from *Angelica pubescens*. Eur J Pharmacol 219: 29-34, 1992.
17. Jiao Y, Kong L, Yao Y, Li S, Tao Z, Yan Y and Yang J: Osthole decreases beta amyloid levels through up-regulation of miR-107 in Alzheimer's disease. Neuropharmacology 108: 332-344, 2016.
18. Wen YC, Lee WJ, Tan P, Yang SF, Hsiao M, Lee LM and Chien MH: By inhibiting snail signaling and miR-23a-3p, osthole suppresses the EMT-mediated metastatic ability in prostate cancer. Oncotarget 6: 21120-21136, 2015.
19. Hu Y, Wen Q, Liang W, Kang T, Ren L, Zhang N, Zhao D, Sun D and Yang J: Osthole reverses beta-amyloid peptide cytotoxicity on neural cells by enhancing cyclic AMP response element-binding protein phosphorylation. Biol Pharm Bull 36: 1950-1958, 2013.
20. Lin VC, Chou CH, Lin YC, Lin JN, Yu CC, Tang CH, Lin HY and Way TD: Osthole suppresses fatty acid synthase expression in HER2-overexpressing breast cancer cells through modulating Akt/mTOR pathway. J Agric Food Chem 58: 4786-4793, 2010.
21. Curtin NJ: Inhibiting the DNA damage response as a therapeutic manoeuvre in cancer. Br J Pharmacol 169: 1745-1765, 2013.
22. Wang Y, Ji P, Liu J, Broaddus RR, Xue F and Zhang W: Centrosome-associated regulators of the G_2/M checkpoint as targets for cancer therapy. Mol Cancer 8: 8, 2009.
23. Dash BC and El-Deiry WS: Phosphorylation of p21 in G_2/M promotes cyclin B-Cdc2 kinase activity. Mol Cell Biol 25: 3364-3387, 2005.
24. Cortese K, Daga A, Monticone M, Tavella S, Stefanelli A, Aiello C, Bisio A, Bellese G and Castagnola P: Carnosic acid induces proteasomal degradation of Cyclin B1, RB and SOX2 along with cell growth arrest and apoptosis in GBM cells. Phytomedicine 23: 679-685, 2016.
25. Zhao XX, Chang JJ, Wang QL, Lu R, Li LJ, Sun X, Xie WD and Li X: 5,6-Dihydroxy-3,7,4'-trimethoxyflavonol induces G2/M cell cycle arrest and apoptosis in human hepatocellular carcinoma cells. J Asian Nat Prod Res 18: 1079-1090, 2016.
26. Wang L, Yang L, Lu Y, Chen Y, Liu T, Peng Y, Zhou Y, Cao Y, Bi Z, Liu T, *et al*: Osthole induces cell cycle arrest and inhibits migration and invasion via PTEN/Akt pathways in osteosarcoma. Cell Physiol Biochem 38: 2173-2182, 2016.
27. Matsunaga T, Mu D, Park CH, Reardon JT and Sancar A: Human DNA repair excision nuclease. Analysis of the roles of the subunits involved in dual incisions by using anti-XPG and anti-ERCC1 antibodies. J Biol Chem 270: 20862-20869, 1995.
28. Evans E, Moggs JG, Hwang JR, Egly JM and Wood RD: Mechanism of open complex and dual incision formation by human nucleotide excision repair factors. EMBO J 16: 6559-6573, 1997.
29. Frich L, Bjørnland K, Pettersen S, Clausen OP and Gladhaug IP: Increased activity of matrix metalloproteinase 2 and 9 after hepatic radiofrequency ablation. J Surg Res 135: 297-304, 2006.
30. Liu B, Cui J, Sun J, Li J, Han X, Guo J, Yi M, Amizuka N, Xu X and Li M: Immunolocalization of MMP9 and MMP2 in osteolytic metastasis originating from MDA-MB-231 human breast cancer cells. Mol Med Rep 14: 1099-1106, 2016.
31. Pietruszewska W, Bojanowska-Poźniak K and Kobos J: Matrix metalloproteinases MMP1, MMP2, MMP9 and their tissue inhibitors TIMP1, TIMP2, TIMP3 in head and neck cancer: An immunohistochemical study. Otolaryngol Pol 70: 32-43, 2016.
32. Gugnoni M, Sancisi V, Gandolfi G, Manzotti G, Ragazzi M, Giordano D, Tamagnini I, Tigano M, Frasoldati A, Piana S, *et al*: Cadherin-6 promotes EMT and cancer metastasis by restraining autophagy. Oncogene: Jul 4, 2016 (Epub ahead of print). doi: 10.1038/onc.2016.237.
33. Ji S, Zhang W, Zhang X, Hao C, Hao A, Gao Q, Zhang H, Sun J and Hao J: Sohlh2 suppresses epithelial to mesenchymal transition in breast cancer via downregulation of IL-8. Oncotarget: Jun 30, 2016 (Epub ahead of print). doi: 10.18632/oncotarget.10355.
34. Sun X, Zhao S, Li H, Chang H, Huang Z, Ding Z, Dong L, Chen J, Zang Y and Zhang J: MicroRNA-30b suppresses epithelial-mesenchymal transition and metastasis of hepatoma cells. J Cell Physiol: Jun 23, 2016 (Epub ahead of print). doi: 10.1002/jcp.25466.
35. Hung CM, Kuo DH, Chou CH, Su YC, Ho CT and Way TD: Osthole suppresses hepatocyte growth factor (HGF)-induced epithelial-mesenchymal transition via repression of the c-Met/Akt/mTOR pathway in human breast cancer cells. J Agric Food Chem 59: 9683-9690, 2011.
36. Kao SJ, Su JL, Chen CK, Yu MC, Bai KJ, Chang JH, Bien MY, Yang SF and Chien MH: Osthole inhibits the invasive ability of human lung adenocarcinoma cells via suppression of NF-κB-mediated matrix metalloproteinase-9 expression. Toxicol Appl Pharmacol 261: 105-115, 2012.